

Quasiparticle Theory versus Density-Functional Theory at a Metal Surface

John J. Deisz*

*Physikalisches Institut, Universität Würzburg, 8700 Würzburg, Germany
and Department of Physics, Montana State University, Bozeman, Montana 59717*

Adolfo G. Eguiluz†

*Fritz-Haber-Institut der Max-Planck-Gesellschaft, 1000 Berlin 33, Germany
and Department of Physics, Montana State University, Bozeman, Montana 59717*

Werner Hanke

*Physikalisches Institut, Universität Würzburg, 8700 Würzburg, Germany
(Received 21 December 1992)*

We report a first-principles comparison between quasiparticle (QP) theory and density-functional theory (DFT) at a jellium surface. Once long-range Coulomb correlations—which are outside the local-density approximation—are incorporated into DFT through the exchange-correlation potential, the same yields wave functions and energy eigenvalues which are excellent approximations to their QP image-state counterparts. By contrast, our results for the electron self-energy near the surface do not support the use of local potentials for the description of excited-state damping.

PACS numbers: 73.20.-r, 71.10.+x

Density-functional theory (DFT) provides a universal scheme for the treatment of Coulomb correlations in solids via the introduction of an exchange and correlation (XC) energy functional $E_{XC}[n]$ and associated XC potential $V_{XC}(\mathbf{x})$ [1,2]. Now as originally formulated, and commonly implemented, DFT is restricted to the ground state of a many-electron system [1]. Thus, in principle, spectroscopic investigations of solids which, by definition, probe electron dynamics, are outside the realm of the theory.

Diagrammatic perturbation theory provides an alternative approach to the many-body problem which is free from this limitation [3]. However, its implementation is substantially more involved than that of DFT, since it requires an explicit self-consistent treatment of the dynamics and nonlocality of the XC process embodied in the electron self-energy $\Sigma_{XC}(\mathbf{x}, \mathbf{x}'|E)$. By contrast, in the numerical implementation of DFT the intricacy of the XC process is largely bypassed (the same is an issue when formulating a theory of the functional $E_{XC}[n]$), and one rigorously deals with a local energy-independent potential.

As a consequence, DFT eigenvalues and wave functions are used in many cases in the interpretation of experiments such as photoemission and inverse photoemission—often with considerable success [4]. It is clearly an important proposition to seek to elucidate the reasons for this *a posteriori* success of DFT, to ascertain the situations where the method fails (e.g., band gaps), and to develop the many-body perturbation theory for the evaluation of observables, such as excited-state lifetimes, which are inherently outside DFT.

In this Letter we compare both approaches to the many-body problem for a metal surface, modeled by jellium. The emphasis is placed on a particularly “extreme”

situation; i.e., we focus on states which are bound by the image tail of the surface barrier—the image states [5–8]. The physics of these states, whose description in DFT requires going beyond the local-density approximation (LDA) [1], is governed by the dual features of long-range Coulomb correlations and strong charge localization at the surface—thus the image states are direct probes of many-body effects at the surface. Our key conclusion is that upon inclusion of long-range correlations the DFT eigenfunctions are extremely good approximations to their quasiparticle (QP) counterparts [9]; furthermore, the QP energy shifts are found to be small. This success of DFT for our prototype inhomogeneous system is interpreted with the aid of an effective local QP potential which we define. Our results have important practical consequences for the implementation of many-body perturbation theory at a surface.

Since the above comparison is in essence one between $\Sigma_{XC}(\mathbf{x}, \mathbf{x}'|E)$ and $V_{XC}(\mathbf{x})$, we also touch on a related and rather general issue, namely, whether the physics of the self-energy near the surface can be simulated by a local potential—a question of relevance in, e.g., electron-surface scattering studies [10]. We find that the damping of the QP states necessitates a nonlocal description; i.e., the inherent nonlocality and energy dependence of the imaginary part of the electron self-energy at the surface precludes a meaningful definition of a complex *local* optical potential.

We discuss the electron self-energy $\Sigma_{XC}(\mathbf{x}, \mathbf{x}'|E)$ first. Since we are particularly interested in image states, what is essential is for Σ_{XC} to incorporate long-range Coulomb correlations. The *GW* approximation [3] fulfills this requirement, and has proved successful in recent self-energy studies in solids [11–14]; thus we adopt it in the present work (effects beyond the *GW* are expected to be

important in strongly correlated Hubbard-like systems):

$$\Sigma_{XC}(\mathbf{x}, \mathbf{x}'|E) = \frac{i}{2\pi} \int dE' e^{iE'\eta} g(\mathbf{x}, \mathbf{x}'|E+E') \times W(\mathbf{x}, \mathbf{x}'|E'), \quad (1)$$

where $g(\mathbf{x}, \mathbf{x}'|E)$ is the QP Green's function and $W(\mathbf{x}, \mathbf{x}'|E)$ is the dynamically screened electron-electron

interaction, $W = v + v\chi_T v$ [3,15], where v is the bare Coulomb interaction and χ_T is the (time-ordered) density response function [16].

The formal basis of the GW scheme is completed by the Dyson equation relating g and Σ_{XC} . Equivalently, the spectrum of QP excitations can be determined by the self-consistent solution of the equation [3]

$$\left[-\frac{\hbar^2}{2m} \nabla^2 + V_{ES}(\mathbf{x}) \right] \Psi_{QP}(\mathbf{x}) + \int d^3x' \Sigma_{XC}(\mathbf{x}, \mathbf{x}'|E_{QP}) \Psi_{QP}(\mathbf{x}') = E_{QP} \Psi_{QP}(\mathbf{x}), \quad (2)$$

where $V_{ES}(\mathbf{x})$ is the electrostatic potential and we have denoted by E_{QP} a (complex) QP energy and by $\Psi_{QP}(\mathbf{x})$ the corresponding QP amplitude (from whose argument we have suppressed the energy eigenvalue to which it corresponds).

We have solved Eq. (2) for a jellium slab [17]. Our solution involves several levels of self-consistency. The QP eigenvalue E_{QP} results from an iterative solution of Eq. (2) starting from an appropriate DFT eigenvalue. In this procedure the dynamical screening process is accounted for self-consistently through the solution of the

integral equation $\chi_T = \tilde{\chi} + \tilde{\chi} v \chi_T$ [3,18], where $\tilde{\chi}$ is the irreducible polarizability. We invoke the random-phase approximation, in which $\tilde{\chi}$ is taken to be the density-response function for noninteracting electrons, χ^0 . The self-consistent electron density profile at the surface is used at all stages. The only simplification made (and the same is justified *a posteriori* by the results discussed below) is the use in Eq. (1) of the DFT Green's function g_0 (computed from DFT eigenvalues and eigenfunctions) in place of the QP Green's function g [11,12].

In Fig. 1 we show the two-dimensional Fourier transform of the self-energy, $\Sigma_{XC}(q_{\parallel} E | z, z')$ (z being the coordinate normal to the surface), for values of the wave vector (parallel to the surface) q_{\parallel} and energy E which correspond to the self-consistent solution of Eq. (2) for the QP image state to be considered below [17]. In Fig. 1(a) the electron is at the jellium edge, $z' = 0$. In this case the nonlocality of both $\text{Re}\Sigma_{XC}$ and $\text{Im}\Sigma_{XC}$, measured by the half-width of the cusp for $z = z'$, is rather modest—a small fraction of a Fermi wavelength.

As the electron leaves the surface the amplitude of the cusp in $\text{Re}\Sigma_{XC}$ can be shown to decay as z^{-1} [19,20]; i.e., it behaves like a classical image potential. A new and dramatic feature of the nonlocality of the self-energy at the surface is illustrated in Fig. 1(b): The maximum in $\text{Im}\Sigma_{XC}$ occurs quite removed from the electron position z' ; i.e., the cusp in $\text{Im}\Sigma_{XC}$ stays at the surface as the electron moves into the vacuum.

We emphasize that *the range of the nonlocality of the cusp of $\text{Im}\Sigma_{XC}$ in the vacuum is comparable with the length over which the electron density decays to zero outside the surface*. Thus, a rigorous description of electron dynamics at a surface requires that Coulomb correlation effects be treated—as we have done—on the same footing with the strong inhomogeneity of the electron density profile at the surface.

Next we compare the predictions of QP theory and DFT for physically significant states, such as image states. The counterpart of Eq. (2) in DFT is the Kohn-Sham (KS) equation [1],

$$\left[-\frac{\hbar^2}{2m} \nabla^2 + V_{ES}(\mathbf{x}) + V_{XC}(\mathbf{x}) \right] \phi_v(\mathbf{x}) = E_v \phi_v(\mathbf{x}), \quad (3)$$

which is solved self-consistently with the electron density. Note that if it were possible to equate the nonlocal self-

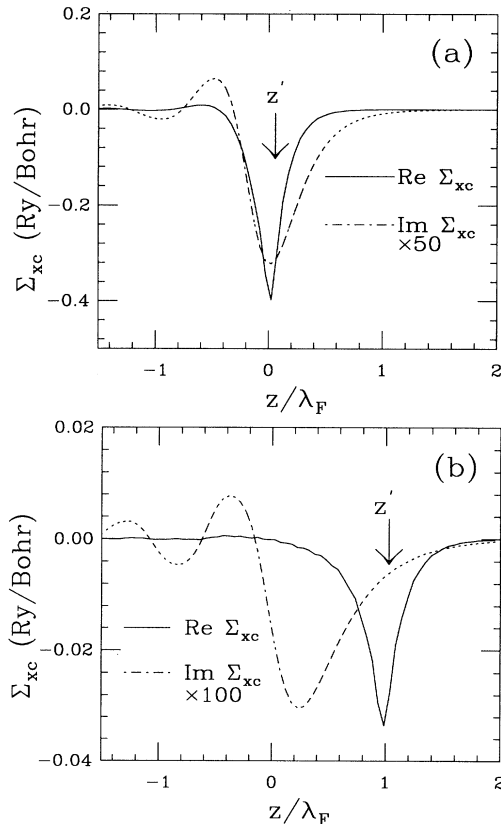


FIG. 1. The electron self-energy Σ_{XC} at a jellium surface with $r_s = 2.07$ for $q_{\parallel} = 0.2k_F$ and $E = 0.3E_F$, values which correspond to the image state shown in Fig. 2 (the energy is measured from the Fermi level). (a) The electron is at the jellium edge. (b) The electron is one Fermi wavelength into the vacuum.

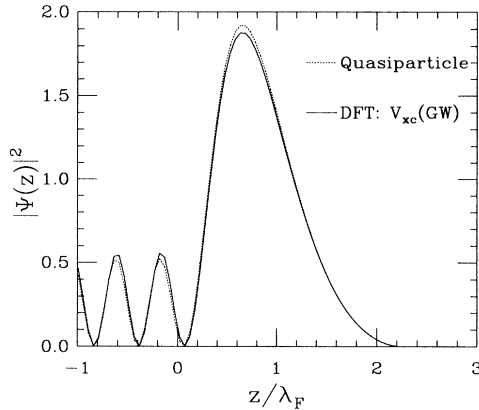


FIG. 2. Comparison of the (modulus square of the) QP amplitude $\Psi_{QP}(z)$ (for the same values of q_{\parallel} and E as in Fig. 1) and the DFT wave function $\phi_v(z)$ (for the same q_{\parallel}) for the $n=1$ image state for a jellium surface with $r_s=2.07$. (See Ref. [21].)

energy Σ_{XC} with the local XC potential V_{XC} , Eq. (2) would reduce to Eq. (3).

Now image states are outside the realm of the LDA, a shortcoming shared by gradient-corrections schemes [2]. Very recently we have developed a method for incorporating long-range Coulomb correlations—and thus image states—into the KS equation [15,21]. Our method is based on obtaining $V_{XC}(z)$ by solving an exact integral equation [22] which relates it to Σ_{XC} (which we evaluate in the *GW*). The solution for $V_{XC}(z)$ is turned into a “nonlocal” XC functional of the electron density for use in Eq. (3) [15,21].

In Fig. 2 we compare the quasiparticle amplitude $\Psi_{QP}(z)$ and the DFT wave function $\phi_v(z)$ —obtained with use of our nonlocal $V_{XC}(n)$ —for the $n=1$ image state, i.e., the lowest-lying solution of Eqs. (2) and (3), respectively, whose existence is due to the long-range image tail of the respective “potential barrier” [23]. Clearly, *although V_{XC} does not mimic the complex structure of the self-energy depicted in Fig. 1, the overlap between the two wave functions is nearly complete (>0.999)*. This result is particularly remarkable in view of the fact that the physics of the present problem is controlled by correlation, while in the bulk, where a similar result has been found [9], correlation plays a smaller role.

The structure of Eqs. (2) and (3) suggests defining an effective local QP potential,

$$U_{\text{eff}}(z) = [\Psi_{QP}(z)]^{-1} \int dz' \Sigma_{XC}(q_{\parallel}E|z, z') \Psi_{QP}(z'), \quad (4)$$

which is such that if the difference $\text{Re}U_{\text{eff}}(z) - V_{XC}(z) \equiv \Delta$ were z independent, we would have that $|\langle \Psi_{QP} | \phi_v \rangle| = 1$, and Δ would be the QP energy shift.

Figure 3(a) shows that Δ is indeed small and nearly z independent [24], which is consistent with the virtual identity of the QP amplitude $\Psi_{QP}(z)$ and DEFT wave function $\phi_v(z)$. The key feature of the integrand of Eq. (4) which leads to this result is not just that the self-

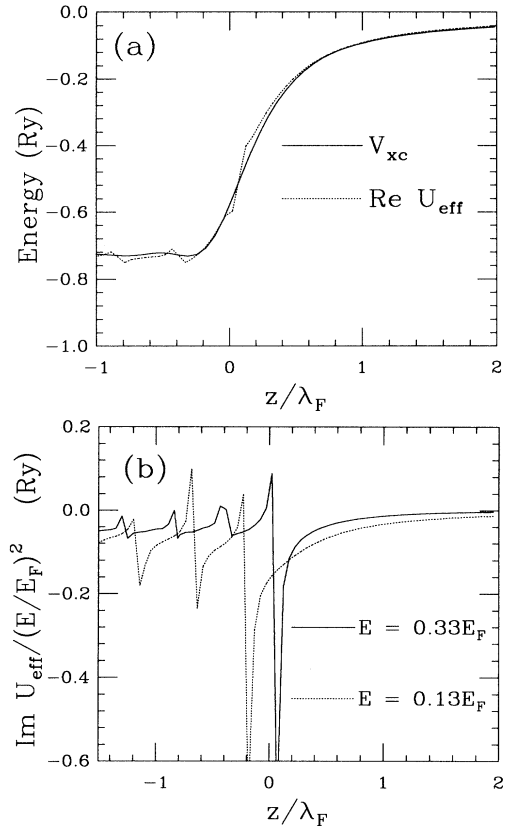


FIG. 3. (a) Comparison of the real part of the effective local QP potential U_{eff} [see Eq. (4)]—for the wave vector and energy given in Fig. 1—and the XC potential V_{XC} . (b) $\text{Im}U_{\text{eff}}$ for two different quasiparticle states (see text). Results refer to a jellium surface with $r_s=2.07$.

energy is integrated over [otherwise similar conclusions would be valid for $\text{Im}U_{\text{eff}}(z)$ —see below], but rather the “weak” nonlocality of $\text{Re}\Sigma_{XC}$, which, in particular, leads to an effective potential (and QP shift Δ) which does not depend sensitively on the QP amplitude used in Eq. (4). [In Fig. 3 $\text{Re}U_{\text{eff}}(z)$ was computed for the $n=1$ image state but (as that result hints at) it does not change much for other states [20].]

The energy difference $E_{QP} - E_v$ is of $O(\Delta)$ and thus small. Specifically, we find $E_{QP} - E_v = 0.02$ eV for $q_{\parallel} = 0$, which is quite small compared to the binding energy of the state—about 0.5 eV. This result should hold for all q_{\parallel} , as the QP effective mass is nearly unity for the homogeneous electron gas [3], and mass-enhancement effects are expected to be even weaker when the electron is far out in the vacuum.

Although there is no counterpart for $\text{Im}U_{\text{eff}}(z)$ in DFT, complex local “optical potentials” are commonly used to account for QP propagation and damping [4,10]. In Fig. 3(b) we show $\text{Im}U_{\text{eff}}(z)$ for two energies which correspond, respectively, to the image-state resonance discussed above ($E=0.33E_F$) and to a surface-truncated bulk state ($E=0.13E_F$). It is clear that simply scaling

the potential for one energy would not yield the potential for the other one. Thus, $\text{Im}U_{\text{eff}}(z)$ depends in a nontrivial way on the state for which it is calculated (and thus on energy as well)—in other words, *in order to construct $\text{Im}U_{\text{eff}}(z)$ one would have to solve the QP problem first.* Clearly this feature of QP propagation inhibits the development of a meaningful prescription for creating local complex potentials out of the more fundamental QP picture.

In addition, unlike the case of $\text{Re}U_{\text{eff}}(z)$ (which, as shown above, agrees well with $V_{\text{XC}}(z)$, a local energy-dependent potential), $\text{Im}U_{\text{eff}}(z)$ is singular near a node of $\Psi_{\text{QP}}(z)$ due to the nonlocality (asymmetry) of $\text{Im}\Sigma_{\text{XC}}$ about $z=z'$. The divergence of $\text{Im}U_{\text{eff}}(z)$ at the first node of $\Psi_{\text{QP}}(z)$ at the surface can be traced to the impact in Eq. (4) of the extreme nonlocality of $\text{Im}\Sigma_{\text{XC}}$ in the vacuum (the explicit energy dependence of $\text{Im}\Sigma_{\text{XC}}$ plays a smaller role).

We note that since our DFT and QP calculations were carried out to the same degree of approximation in the electron-electron interaction—built into the theory through the *GW* self-energy—it seems plausible that our results are intrinsic to the many-body problem. Thus we expect our conclusions to be valid for more elaborate self-energies.

In summary, we have found that upon going beyond LDA by incorporating long-range correlations into $V_{\text{XC}}(n)$, DFT gives an accurate approximation to the QP wave functions for our model strongly inhomogeneous system. Since a similar result has been reported for a very different electronic environment [9]—LDA wave functions at the gap in a bulk semiconductor—this feature of the DFT wave functions may be generic. In addition, we have found that the quasiparticle energy shifts for the image states are small. Both conclusions, which are of obvious impact in simplifying the implementation of diagrammatic perturbation theory at surfaces, are nontrivial, as “nonuniversal” (short-range) features of the surface barrier can lead to binding energy changes of up to 0.2 eV for $n=1$ image states [7]. Finally, we have shown that the large nonlocality of the imaginary part of the electron self-energy outside the surface cannot be accounted for in a meaningful way by a complex local potential.

J.J.D. acknowledges partial support from the Deutscher Akademischer Austauschdienst. A.G.E. acknowledges support from NSF Grant No. DMR-9207747, the San Diego Supercomputer Center, and Cray Research, Inc. W.H. acknowledges support from BMFT Grant No. 03-HA3WUE. A.G.E. and W.H. acknowledge support from NATO.

*Current address: Department of Physics, Georgetown University, Washington, DC 20057.

†Current address: Department of Physics and Astronomy, The University of Tennessee, Knoxville, TN 37996-1200.

[1] P. Hohenberg and W. Kohn, Phys. Rev. **136**, B864 (1964); W. Kohn and L. J. Sham, Phys. Rev. **140**, A1133

(1965).

- [2] See, e.g., R. M. Dreizler and E. K. U. Gross, *Density Functional Theory: An Approach to the Quantum Many-Body Problem* (Springer-Verlag, Berlin, 1990).
- [3] L. Hedin and S. Lundqvist, in *Solid State Physics*, edited by H. Ehrenreich, F. Seitz, and D. Turnbull (Academic, New York, 1969), Vol. 23, p. 1.
- [4] J. E. Inglesfield and E. W. Plummer, in *Angle Resolved Photoemission, Theory and Current Applications*, edited by S. D. Kevan (Elsevier, Amsterdam, 1992), p. 15.
- [5] P. M. Echenique and J. B. Pendry, Prog. Surf. Sci. **32**, 11 (1990).
- [6] F. J. Himpsel, Phys. Rev. B **43**, 13394 (1991); N. V. Smith, Rep. Prog. Phys. **51**, 1227 (1988); V. Dose, Surf. Sci. Rep. **5**, 337 (1985).
- [7] N. Fischer, S. Schuppler, Th. Fauster, and W. Steinmann, Phys. Rev. B **42**, 9717 (1990).
- [8] S. Yang, R. A. Bartynski, G. P. Kochanski, S. Papadia, T. Fondén, and M. Persson (to be published); W. L. Schaich, Phys. Rev. B **45**, 3744 (1992).
- [9] M. S. Hybertsen and S. G. Louie, Phys. Rev. B **38**, 4033 (1988).
- [10] D. L. Mills and S. Y. Tong, Philos. Trans. R. Soc. London A **318**, 1179 (1986).
- [11] L. R. W. Godby, M. Schlüter, and L. J. Sham, Phys. Rev. Lett. **56**, 2415 (1986).
- [12] W. Hanke and L. J. Sham, Phys. Rev. B **38**, 13361 (1988).
- [13] E. Northrup, M. S. Hybertsen, and S. G. Louie, Phys. Rev. Lett. **66**, 500 (1991).
- [14] W. von der Linden and P. Horsch, Phys. Rev. B **37**, 8351 (1988).
- [15] A. G. Eguiluz, M. Heinrichsmeier, A. Fleszar, and W. Hanke, Phys. Rev. Lett. **68**, 1359 (1992).
- [16] In the evaluation of Σ_{XC} we performed numerical integrations over *both* imaginary—and real—energy axes.
- [17] The numerical results presented in Figs. 1–3 correspond to the bulk density $r_s=2.07$ and wave vector $q_{\parallel}=0.2k_F$. We have verified that these results are representative of the physics of the problem; i.e., they are valid for other values of r_s and q_{\parallel} .
- [18] A. G. Eguiluz, Phys. Rev. B **31**, 3305 (1985); Phys. Scr. **36**, 651 (1987).
- [19] J. Rudnik, Ph.D. thesis, University of California, San Diego, 1970 (unpublished).
- [20] J. Deisz and A. G. Eguiluz, J. Phys. Condens. Matter (to be published).
- [21] A. G. Eguiluz, J. J. Deisz, M. Heinrichsmeier, A. Fleszar, and W. Hanke, Int. J. Quantum Chemistry: Quantum Chem. Symposium **26**, 837 (1992). This conference proceedings article contains preliminary discussions of a subset of the material of the present paper. (We note that in Ref. [21] the equation for the QP amplitudes—Eq. (2)—was not solved, unlike the present work.)
- [22] L. J. Sham and M. Schlüter, Phys. Rev. Lett. **51**, 1888 (1983).
- [23] In the absence of a band gap, the image states at a jellium surface are *resonances* (Ref. [15]); Fig. 2 shows a typical $\phi_v(z)$ belonging to a group of closely spaced eigenvalues.
- [24] The jagged features in $U_{\text{eff}}(z)$ inside the jellium are due to the nodes in $\Psi_{\text{QP}}(z)$.